

Gauge Invariant Monopoles in Lattice SU(2) Gluodynamics.

F.V. Gubarev

*Institute of Theoretical and Experimental Physics,
B.Chermushkinskaya 25, Moscow, 117259, Russia*

Abstract

We consider lattice implementation of the recently proposed gauge invariant definition of the monopole charge. Because of the lattice discretization the algorithm gives rise to specific lattice artifacts and an effective Ising model. The Ising-model problem might in principle be solved and we discuss the role of the Maximal Abelian gauge in this respect. The lattice artifacts are much more difficult to deal with since they are mixed up with monopoles thus obscuring the physical observables. Nevertheless, it is possible to extract the density of physical monopoles which seems to scale correctly towards the continuum limit.

Introduction

In this paper we implement the gauge invariant monopole construction [1] on the lattice. Since we use heavily the results of Ref. [1] let us recall first the essentials of the monopole definition in the continuum limit.

One starts with consideration of the fundamental Wilson loop $W(T)$, $\frac{1}{2} \text{Tr} W(T) = \cos \varphi(T)$ calculated on a closed contour $\mathcal{C}(t)$, $t \in [0; T]$. For a given $W(t)$ it is always possible to find a family of spin coherent states $|\vec{n}(t)\rangle$ such that

$$e^{i\varphi(t)} |\vec{n}(t)\rangle = W(t) |\vec{n}(0)\rangle, \quad \vec{n}(T) = \vec{n}(0). \quad (1)$$

Eq. (1) naturally assigns the unique (up to the sign, see below) vector $\vec{n}(t)$ to each point on the contour \mathcal{C} . In terms of $\vec{n}(t)$ the phase angle $\varphi(T)$ of the Wilson loop can be expressed as

$$\varphi(T) = \frac{1}{2} \int_{\mathcal{C}} \vec{A} \vec{n} + \frac{1}{4} \int_{S_{\mathcal{C}}} \vec{n} \cdot \partial \vec{n} \times \partial \vec{n}, \quad (2)$$

where $S_{\mathcal{C}}$ is an arbitrary surface spanned on \mathcal{C} and \vec{A} denotes the tangential to \mathcal{C} components of the gauge potentials, $A^a(t) = A^a_{\mu}(x(t)) \dot{x}_{\mu}(t)$. As is clear from Eq. (1), the initial state $|\vec{n}(0)\rangle$ is an eigenstate of the full Wilson loop. Since $W(T)$ has two eigenstates $|\pm \vec{n}(0)\rangle$ ('spin up' and 'spin down'), with the corresponding families $\pm \vec{n}(t)$ and phases $\pm \varphi(T)$, there is a sign ambiguity in Eq. (1).

One considers next an arbitrary smooth closed surface S^2_{phys} and covers it with a set of infinitesimal patches of area $\delta\sigma_x$. The phase evaluated on each patch is:

$$\delta\varphi_x = \frac{1}{4} \{ \partial \wedge (\vec{n} \vec{A}) + \vec{n} \cdot \partial \vec{n} \times \partial \vec{n} \} \delta\sigma_x. \quad (3)$$

One can show that the usual assumption of the gauge fields continuity implies existence of a smooth field $\vec{n}_x \in S^2_{phys}$. Therefore it is legitimate to integrate Eq. (3) over the surface S^2_{phys} :

$$q = \frac{1}{2\pi} \oint_{S^2_{phys}} \delta\varphi = \frac{1}{8\pi} \oint_{S^2_{phys}} \{ \partial \wedge (\vec{n} \vec{A}) + \vec{n} \cdot \partial \vec{n} \times \partial \vec{n} \} \delta\sigma, \quad (4)$$

and get a gauge invariant definition of the monopole charge contained inside S^2_{phys} . Note that for a smooth S^2_{phys} and for continuous gauge fields the sign ambiguity mentioned above is not important. In fact, it reduces to the freedom to globally change the sign of $\vec{n} \in S^2_{phys}$ which in turn is equivalent to changing the sign of q , see Eq. (4).

One can show [1] that at the classical level it is the singular Wu-Yang monopole solution [2] which corresponds to a non-trivial q . In other words, Eq. (4) provides us with a gauge invariant topological definition of the Wu-Yang monopole which can be used at the quantum level as well. Moreover, the quantum generalization of the Wu-Yang monopole may look quite different from its classical counterpart. Indeed, the classical Wu-Yang solution is unstable [3]. Thus, the semi-classical approximation would be inconsistent. However, the instability of the Wu-Yang solution implies only that monopoles (4) are

irrelevant at short distances $r \ll \Lambda_{QCD}$. As far as the infrared region is concerned the dynamics of the monopoles (4) cannot be treated analytically (see also Ref. [4]). One concludes, therefore, that at the quantum level the field configurations with a non-trivial charge q have little to do with the classical Wu-Yang solution both at short and large distances. Moreover, there seem to be no analytical tools to investigate their dynamics.

Below we discuss the monopole definition (4) on the lattice. Lattice implementation of the continuum ideas is not always straightforward. A particular example is provided by instantons: while in the continuum limit instantons are relatively simple objects, their lattice definition is technically much more involved [5]. Still, in principle, one may try to interpolate the lattice gauge fields and apply the continuum ideas to the interpolated gauge potentials. A drawback of this approach is that the interpolation is always not unique.

Because of the lattice discretization one cannot completely avoid interpolations while implementing Eq. (4) on the lattice. However, our interpolation procedure is unique and not applied to the gauge fields themselves. Instead we interpolate the states $|\vec{n}\rangle$ in between neighboring lattice cells thus getting a continuous field \vec{n} as required by Eq. (4). This enables us to construct integer valued conserved monopole currents on the lattice.

There are two disadvantages of our approach both of which we discuss in detail later:

i) The sign ambiguity mentioned above which is harmless in the continuum reemerges on the lattice in the form of an effective Ising model. In turn, the problem of finding the gauge invariant monopoles on the lattice becomes equivalent to finding the global minima of the corresponding Ising action, which is non-trivial because the model is frustrated. What is surprising, however, is that in the Maximal Abelian gauge the ground state of the Ising model is approximated very well, although we do not fix any particular gauge neither in our construction nor in the numerical simulations.

ii) The interpolation of spin states in between neighboring lattice cells enforces a change of the lattice geometry. Namely, one has to consider additional three dimensional cells on the lattice which can contain gauge invariant monopole charges. We argue below that these charges are pure lattice artifacts which disappear in the limit of infinitesimal lattice spacing. The artifact's contribution to the physical observables must be carefully subtracted which is a non-trivial problem because of complicated lattice geometry and monopole-artifact mixing. Nevertheless, for simple quantities like monopole density the monopole-artifact separation turns possible. When this is done, the density of physical monopoles scales correctly towards the continuum limit.

1. 'Stokes Theorem'

Complexity of the lattice implementation of Eq. (4) might already be visualized from that equation itself. Indeed, the effective 'Higgs field' \vec{n} is unusual since it is defined not on space-time points (lattice sites) but on elementary two-dimensional cells (plaquettes). Moreover, the field \vec{n} is defined [1] in terms of the field strength tensor $F_{\mu\nu}^a$ which itself is badly defined on the lattice. Indeed, in the continuum limit the Wilson loop calculated on a plaquette reduces to a particular component of $F_{\mu\nu}$ regardless of the initial point from

which we started evaluation of Wilson loop. But for a finite lattice spacing the Wilson loop depends drastically on the starting point. Because of this, the spin state which we would like to assign to a given plaquette also depends on the plaquette definition.

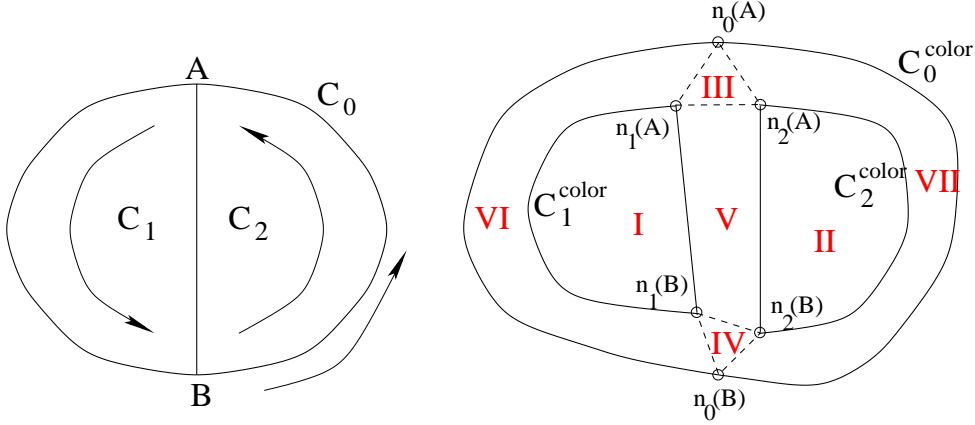


Fig. 1

The situation becomes even worse if we consider a common link of two plaquettes. The spin states are to be constructed on each plaquette separately and they have nothing in common, in contrast with the continuum case. To get insight into the problem, let us consider an arbitrary contour \mathcal{C}_0 and dissect it in points A and B into two smaller pieces \mathcal{C}_1 and \mathcal{C}_2 (Fig. 1). The spin states are introduced for each contour via Eq. (1) taking for definiteness the 'spin up' initial states. In this way one gets three different families $\vec{n}_i(t)$ associated with each contour \mathcal{C}_i . Suppose that we know the phases φ_i of the Wilson loops calculated on \mathcal{C}_i . What is the relation between them?

The answer may be found by considering the image of each contour under the map: $\vec{n}_i : \mathcal{C}_i \rightarrow \mathcal{C}_i^{color}$. Note that the two triples $\{\vec{n}_i(A)\}$, $\{\vec{n}_i(B)\}$, $i = 0, 1, 2$ are distinguishable since the relative position of the vectors in each triple is gauge invariant. Moreover, there exists a simple interpretation of the original Wilson loops in terms of \mathcal{C}_i^{color} . Namely, $W_i(t)$ describes periodic motion of a point-like charged particle on S_{color}^2 since every closed path \mathcal{C}_i^{color} is associated with a unique phase factor. Therefore, in terms of \mathcal{C}_i^{color} the problem becomes essentially Abelian and one could have concluded that φ_0 is equal to the sum of phases calculated on the pre-images of the closed paths I, II, ..., VII (see Fig. 1). But there is a loophole in this argumentation: we do not know the $SU(2)$ matrices g_{ij} which connect the points $\vec{n}_i \rightarrow \vec{n}_j$:

$$g_{ij}(A) : \vec{n}_i(A) \rightarrow \vec{n}_j(A), \quad g_{ij}(B) : \vec{n}_i(B) \rightarrow \vec{n}_j(B) \quad (5)$$

and which are denoted by dashed lines on the Fig. 1. Clearly, g_{ij} might be an arbitrary $SU(2)$ elements provided that Eq. (5) holds true.

Among various $g \in SU(2)$ which connect two given points $\vec{n}_1, \vec{n}_2 \in S_{color}^2$, $g|\vec{n}_1\rangle \sim |\vec{n}_2\rangle$ there is a special one. Namely, if g describes the motion $\vec{n}_1 \rightarrow \vec{n}_2$ along the shortest geodesic connecting \vec{n}_1, \vec{n}_2 then g is uniquely defined:

$$g = (\vec{n}_1 \vec{n}_2) + i\sigma^a [\vec{n}_1 \times \vec{n}_2]^a. \quad (6)$$

We call it the geodesic matrix below. Moreover, for the geodesic matrices g_{ij} the relation between the phases φ_i becomes extremely simple. Indeed, one can readily verify that in this case the phase angles associated with cells V, VI, VII are vanishing while for the cells III, IV they are equal to the oriented areas of the spherical triangles $\{\vec{n}_i(A)\}$ and $\{\vec{n}_i(B)\}$, respectively. Thus, we get the following simple equation which relates the phases of the Wilson loops:

$$\varphi_0 = \varphi_1 + \varphi_2 + \gamma(A) + \gamma(B), \quad (7)$$

$$\gamma(N) = \text{oriented solid angle between } \vec{n}_0(N), \vec{n}_1(N), \vec{n}_2(N).$$

Note that we always implicitly assume mod 2π operation [1].

2. Single Plaquette Construction.

We start the construction of monopoles (4) on the lattice following the same strategy as in the continuum limit. Namely, the simplest object which we consider first is an elementary plaquette, see Fig. 2.

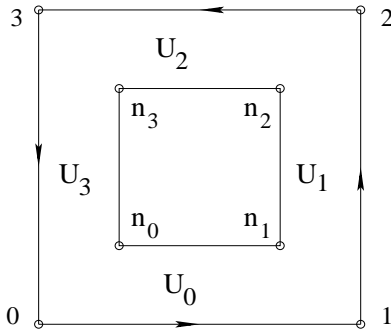


Fig. 2

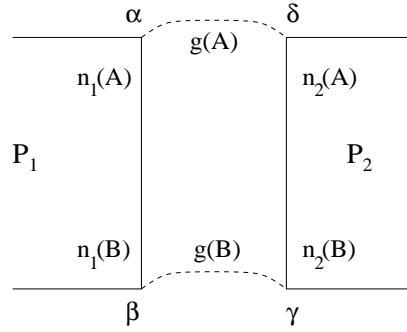


Fig. 3.

As is noted above for any finite lattice spacing the matrix $U_p = U_1 U_2 U_3 U_4$ is to be treated as a large Wilson loop. In particular, it is impossible to assign a single well defined spin state to a given plaquette. On the other hand, the Eq. (1) is still valid and in fact directly applicable. Namely, one can calculate the eigenvector of the matrix U_p :

$$\langle \vec{n}_0 | U_p = e^{i\varphi_p} \langle \vec{n}_0 | \quad (8)$$

and then propagate the initial state $\langle \vec{n}_0 |$ along the plaquette's edges:

$$\langle \vec{n}_k | U_k = e^{i\varphi_k} \langle \vec{n}_{k+1} |, \quad k = 0, \dots, 3, \quad \langle \vec{n}_4 | = \langle \vec{n}_0 |. \quad (9)$$

In this way one gets four states $\langle \vec{n}_k |$ sitting at the plaquette's corners. Moreover, each $\langle \vec{n}_k |$ is an eigenstate of the plaquette matrix calculated starting from point k , e.g. $\langle \vec{n}_1 | U_1 U_2 U_3 U_0 \sim \langle \vec{n}_1 |$ etc. Therefore, the vectors \vec{n}_k are in a sense always parallel to the color magnetic field piercing the plaquette considered. Moreover, Eqs. (8,9) imply the

following simple relation between the plaquette angle φ_p and phases φ_i associated with the corresponding links:

$$\varphi_p = \sum_{k=0}^3 \varphi_k. \quad (10)$$

Note that we still have a freedom to choose an arbitrary sign of the initial state (8), the same as in the continuum limit. It is clear that the change $\vec{n}_0 \rightarrow -\vec{n}_0$ would also flip the signs of all other states: $\vec{n}_k \rightarrow -\vec{n}_k$. Thus, it makes sense to speak about the sign associated with each plaquette. While only a single plaquette is considered the sign ambiguity is in fact irresolvable. Note also that for pure diagonal link matrices all vectors \vec{n}_k collapse to a single point on the S_{color}^2 .

Next, consider a common link of two adjacent plaquettes, see Fig. 3. Since the spin states are constructed separately on each plaquette the states $\vec{n}_1(A)$, $\vec{n}_2(A)$ and $\vec{n}_1(B)$, $\vec{n}_2(B)$ are quite different in general. It is important, however, that the products $\vec{n}_1(A) \cdot \vec{n}_2(A)$ and $\vec{n}_1(B) \cdot \vec{n}_2(B)$ are gauge invariant. Moreover, in case of diagonal lattice gauge fields (or for a gauge copy of the diagonal configuration) we have

$$\vec{n}_1(A) \cdot \vec{n}_2(A) = \vec{n}_1(B) \cdot \vec{n}_2(B) = \pm 1, \quad (11)$$

depending on the relative sign of initial states chosen on each plaquette. Therefore, there is a natural way to fix the relative sign on P_1 and P_2 by the requirement that across the common link of two plaquettes the spins should be as smooth as possible. In fact, this approach is essentially the same as in the continuum limit. The only difference is that in the continuum we indeed do have a continuous distribution of spins while on the lattice the true smoothness of \vec{n}_x is not possible. The only exception is a particular case $|\vec{n}_1(A) \cdot \vec{n}_2(A)| = 1$ for which everything is in fact trivial.

Thus, on the lattice we inevitably have to interpolate the states $\vec{n}_1(A)$ and $\vec{n}_2(A)$ by connecting them with an appropriate $SU(2)$ matrix g such that $\langle \vec{n}_1 | g \sim \langle \vec{n}_2 |$. As we have argued in the previous section there is a natural unique choice of g , namely the geodesic interpolation, Eq. (6). This choice is singled out, in particular, since only in this case we do not introduce additional fluxes in the intersection of two plaquettes: the Wilson loop calculated on 2-cell $(\alpha\beta\gamma\delta)$ is exactly unity no matter what the lattice gauge fields are.

3. Monopole Charge on 3D Cube.

The above construction allows to formulate the notion of the monopole charge for a single three-dimensional lattice cube. Namely, one has to apply the procedure of the previous section to all six plaquettes of a given cube, Fig. 4.

Let us briefly summarize the essential steps of the construction.

i) On each face $\alpha = 0, \dots, 5$ of the cube one calculates the corresponding plaquette matrix U_α and then constructs four vectors $\vec{n}_{i,\alpha}$, $i = 0, \dots, 3$ via Eq. (9) taking the initial state $\vec{n}_{0,\alpha}$ as an eigenstate of U_α with arbitrary sign.

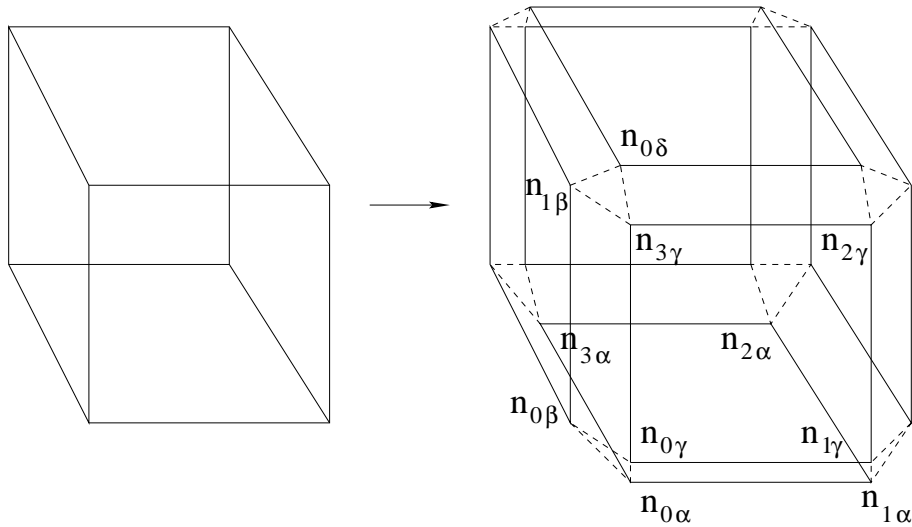


Fig. 5

ii) In order to get the smoothest distribution of $\vec{n}_{i,\alpha}$ on the cube boundary, one considers the following Ising-like action:

$$S = - \sum_{\alpha\beta} z_\alpha z_\beta \sum_{i,j} \vec{n}_{i,\alpha} \cdot \vec{n}_{j,\beta}, \quad (12)$$

where dynamical variables are the signs $z_\alpha = \pm 1$ associated with each plaquette, the first sum is over all neighboring 2-cells in the cube's boundary and the summation in i, j indexes extends over all neighboring spins. The action (12) is minimized with respect to all signs z_α and, finally, for negative z_α the corresponding vectors $\vec{n}_{i,\alpha}$ are inverted $\vec{n}_{i,\alpha} \rightarrow -\vec{n}_{i,\alpha}$. It is clear that the ground state of the Ising model (12) corresponds to the smoothest possible distribution of $\vec{n}_{i,\alpha}$. Moreover, for a single cube the ground state may be found exactly.

iii) Finally, the three vectors around each vertex of the cube are geodesically interpolated (dashed lines on Fig. 5). Note that the relative position of vectors in each triple, say $(\vec{n}_{1,\beta}, \vec{n}_{3,\gamma}, \vec{n}_{0,\delta})$ is gauge invariant and therefore the geodesic interpolation is a well defined prescription.

The magnetic charge contained in a given cube is proportional to the net outgoing magnetic flux, cf. Eq. (4). Namely, one sums up the phases φ_i associated via Eq. (8) with all two-dimensional cells on the boundary of the 'extended' cube (Fig. 5, right). Note that due to the geodesic interpolation not all the 2-cells must be taken into account. For example, the flux emanating through the 2-cell $(\vec{n}_{1,\beta}, \vec{n}_{0,\beta}, \vec{n}_{0,\gamma}, \vec{n}_{3,\gamma})$ is exactly zero. The final expression for the magnetic charge is therefore

$$q = \frac{1}{2\pi} \left[\sum_{\text{plaq } \alpha=0}^5 \varphi_\alpha + \sum_{\text{vertex } v=0}^7 \tilde{\varphi}_v \right], \quad (13)$$

where φ_α is the plaquette angle (8) and $\tilde{\varphi}_v$ is the flux corresponding to the triangle (dashed

lines) at vertex v which in turn is equal to the oriented solid angle between vectors $\vec{n}_{i,\alpha}$ at the triangle's corners.

Eq. (13) has in fact a transparent meaning. The first term counts the flux emanating through the original lattice plaquettes and therefore it is the physical flux of the monopole. The second term is in a sense a correction due to the lattice coarseness. Indeed, there were two important requirements in the corresponding continuum construction : S_{phys}^2 should be smooth and $\delta\varphi_x$ is to be calculated on an infinitesimal contour $\delta\mathcal{C}_x$. In fact none of them is realized on the lattice since the lattice cube for sure cannot be considered as a smooth surface and the lattice plaquette is not infinitesimal in any sense. In fact the second term in Eq. (13) just accounts for these facts by plugging the holes between the neighboring vectors \vec{n}_x . Let us emphasize that the appearance of the additional contribution, Eq. (13), is entirely due to the lattice discretization. There are no similar term in the continuum expression (4).

However, there exists a particular case when the second contribution, Eq. (13), is zero. This happens when all the neighboring spins $\vec{n}_{i,\alpha}$ are aligned with each other. From Eq. (11) we conclude then that this corresponds to a pure Abelian configuration. Namely, there exists a particular gauge in which all the lattice gauge fields are diagonal. Moreover, Eq. (13) is then identical to the well known DeGrand–Toussaint definition of the Abelian monopole [6].

4. Effective Ising Model and Lattice Artifacts.

In this section we discuss some details of the above construction which are in fact crucial in the actual numerical implementations. For simplicity, we consider in this section three dimensional lattice only. Let us start from the Eq. (12) which encodes the way how to get the smoothest possible distribution of spins $\vec{n}_{i,\alpha}$. In fact, it is quite important to find the global minimum of the action (12). Indeed, let us consider an almost Abelian gauge fields configuration for which

$$n_{i,\alpha}^a \approx \pm \delta^{a3} \quad \forall i, \alpha. \quad (14)$$

Suppose that instead of the ground state of the model (12) we are considering a local minimum of the action (12). After performing the corresponding inversions $\vec{n}_{i,\alpha} \rightarrow -\vec{n}_{i,\alpha}$ for all the negative z_α we get a configuration of vectors $\vec{n}_{i,\alpha}$ almost all of which satisfy $\vec{n}_{i,\alpha} \approx \delta^{a3}$. But since the minimum is only local there are some negative spins as well. Evidently, Eq. (13) when applied for such $\{\vec{n}_{i,\alpha}\}$ still produces a non zero charge which however has nothing to do with reality since the contribution comes mostly from the second term of Eq. (13).

Therefore, it is indeed important to find the true ground state of the model (12) before applying Eq. (13). One expects, however, that in the real simulations it is almost impossible to find the global minima since for non-Abelian gauge fields the model (12) is frustrated. Thus the concrete algorithm used to minimize (12) might be crucial.

As a matter of fact, the naive local minimization of (12) is doomed to produce unphysical results for the monopoles (13). One may try to improve the iterative minimization

by preconditioning it with a particular gauge fixing of the original lattice gauge fields. In our numerical tests (see below) we have considered three particular gauge fixing prescriptions: minimal and center Landau and Maximal Abelian gauges which are defined via maximization of the following functionals

$$\sum_l \frac{1}{2} \text{Tr } U_l, \quad \sum_l \left(\frac{1}{2} \text{Tr } U_l \right)^2, \quad \sum_l \frac{1}{2} \text{Tr } U_l \sigma^3 U_l^+ \sigma^3, \quad (15)$$

respectively. Our finding is that the Maximal Abelian gauge is indeed greatly favored¹. Namely, when the lattice fields are first MAA gauge fixed then for each α it is sufficient to pick up the nearest to the north pole family $\vec{n}_{i,\alpha}$. The resulting distribution $\{\vec{n}_{i,\alpha}\}$ almost exactly corresponds to the ground state of (12). For other gauges the result is less pronounced: although Landau gauge fixing improves the local minimization the resulting minimal value of (12) is considerably larger than in case of the Maximal Abelian gauge.

Let us note that in our numerical simulations none of the gauges (15) was used. Instead, we have applied a variant of the simulated annealing algorithm [7] to directly minimize the action (12). As one may expect the latter approach turns out to be superior to any kind of local minimization.

Let us turn now to another major problem of the lattice implementation of Eq. (4). Namely, one can see that Fig. 5 implies in fact a change of the lattice geometry since this construction being iterated for all 3-cubes produces 'extended' cubes instead and introduces new three dimensional cells on the lattice. In particular, in the intersection of four cubes one gets the geometrical figure depicted on the Fig. 6 and a new 3-cell at each site of the original lattice, see Fig. 7.

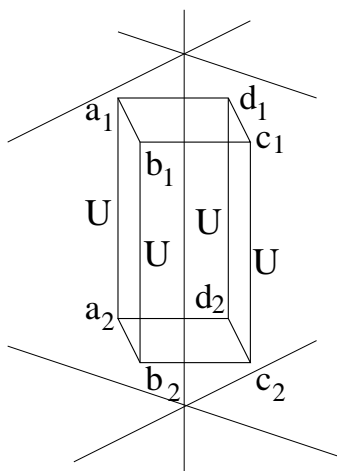


Fig. 6

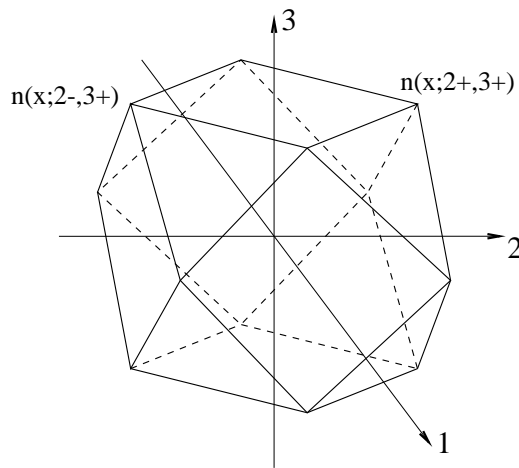


Fig. 7

Consider first the Fig. 6. For the plotted 3-cell the faces $(a_i b_i c_i d_i)$, $i = 1, 2$ consist of the geodesic matrices while all others were in fact already discussed. Namely we have shown

¹ See the next section for details on numerics.

that fluxes piercing the cells $(b_1 b_2 c_2 c_1)$, (a_1, a_2, b_1, b_2) etc. are exactly zero. Moreover, since there is the same matrix U on each link $(a_1 a_2)$, $(b_1 b_2)$ etc. one concludes that the images of squares $(a_i b_i c_i d_i)$, $i = 1, 2$ under the maps $\vec{n}(a_i)$, $\vec{n}(b_i)$ etc. are isomorphic. Due to the properties of the geodesic interpolation the fluxes piercing $(a_1 b_1 c_1 d_1)$ and $(a_2 b_2 c_2 d_2)$ are exactly the same.

The overall conclusion about Fig. 6 is as follows. The magnetic charge inside the plotted 3-cell is identical zero. Moreover, the flux which goes from this cell to the neighboring cubes is zero either. The whole flux propagates unmodified along the link of the original lattice from the face $(a_1 b_1 c_1 d_1)$ to the face $(a_2 b_2 c_2 d_2)$, see Fig. 6.

Turn now to the 3-cell on the Fig. 7. Its properties are easy to derive. Namely, at each vertex there is a corresponding vector \vec{n}_i , $i = 0, \dots, 11$. It is convenient to parameterize the vertices as $(x; \hat{\mu}, d_\mu; \hat{\nu}, d_\nu) \equiv (x; \hat{\nu}, d_\nu; \hat{\mu}, d_\mu)$, where $\hat{\mu}$, $\hat{\nu}$ are the unit vectors along the lattice axes and d_μ , d_ν are the corresponding shift signs (see Fig. 7). Moreover, the pairs of vertices

$$(x; \hat{\mu}, d_\mu; \hat{\nu}, d_\nu), (x; \hat{\mu}, d_\mu; \hat{\lambda}, d_\lambda) \quad \forall \mu, \nu, \lambda$$

are connected by a link which carries an $SU(2)$ matrix g such that

$$g : \vec{n}(x; \hat{\mu}, d_\mu; \hat{\nu}, d_\nu) \rightarrow \vec{n}(x; \hat{\mu}, d_\mu; \hat{\lambda}, d_\lambda)$$

corresponds to the geodesic motion on S_{color}^2 . Note that the relative position of all $\vec{n}(x; \hat{\mu}, d_\mu; \hat{\nu}, d_\nu)$ is gauge invariant and therefore the construction of the 3-cell on the Fig. 7 is well defined.

From the above properties one concludes that fluxes emanating from the faces of the presented 3-cell are equal to the oriented solid angles between the corresponding vectors situated at the vertices of that face. Then it follows immediately that the magnetic charge inside this 3-cell is gauge invariant and in general non-zero. Thus, we get another type of monopoles which however live in the sites of original lattice contrary to the monopoles in Eq. (13), which belong to the dual lattice, as usual. In fact, there is another striking property of the monopoles on the Fig. 7. Namely, none of the fluxes which this monopole emanates enter the original Wilson action of the lattice gauge models. Therefore, naively this monopole costs no action at all.

One can readily convince oneself that the actionless monopoles are of the same origin as the second term in Eq. (13). They appear because of the violation on the lattice of the two major requirements of continuum theory (see the discussion after Eq. (13)). We conclude, therefore, that the actionless monopoles are intrinsic to the lattice formulation. They disappear only in the academic limit of such small lattice spacing that one can indeed identify the lattice plaquette with a particular component of continuum $F_{\mu\nu}$. Of course, in this limit the above single cube construction is not applicable any longer and one has to consider the extended monopoles [8].

Thus, the actionless monopoles are in fact lattice artifacts which exist only because of the lattice discretization. When any physical observable is measured on the lattice the contribution of this objects must be carefully subtracted – the task which is quite non-trivial by itself. Indeed, even if $D = 3$ and the lattice geometry is well understood

(see Figs. 5-7) there seems to be no unique way to extract, e.g., density of the physical monopoles. In three dimensions the monopoles are point-like and one may naively expect that each artifact should form a small dipole-like structure either with 'physical' monopole or with another artifact. But this expectation is in fact wrong since the flux emanating from each artifact is not suppressed by the action. Therefore, e.g., artifact-artifact chain might be arbitrarily prolonged.

In four dimensions the situation is even worse because of the complicated lattice geometry. The monopole currents are of course conserved, but the conservation takes place not on the hypercubical lattice. As a result the monopoles may freely propagate from 3-cubes to the sites and back on the original lattice. Thus, discrimination against the artifacts becomes ambiguous. Nevertheless in the next section we show that in $D = 4$ the simplest 'brute-force' approach works unexpectedly well for the monopole density.

We also would like to mention that there exists another view on the monopole-artifact mixing. Indeed, suppose for a while that the second term in Eq. (13) is zero. Then the monopole and artifact currents are separately conserved on the hypercubical dual and original lattices, respectively, and therefore there is no mixing between them. Thus it is the second term in Eq. (13) which mixes together the two types of magnetic charges.

Finally, let us note that there might be another way to fight against the artifacts on the lattice. Here we mean in particular a kind of blocking procedure which preserves the infrared properties of the theory while filtering out the ultraviolet noise. This might be helpful in approaching the limit of infinitesimal lattice spacing where the artifacts for sure disappear.

5. Results of Numerical Simulations.

In this section we describe the results of our numerical simulations of the four dimensional pure $SU(2)$ lattice gauge model. We have noted already that it is in fact crucial to have a good approximation to the ground state of the model (12) which amounts to the ability to approximate the global minima of the corresponding action. We have considered three different types of minimization procedure, namely, the naive local minimization with and without gauge fixing preconditioning and a variant of the simulated annealing algorithm.

The gauges considered were described above, see Eq. (15), and each gauge was fixed by the iterative maximization of the corresponding functional. The gauge was considered fixed when all gauge rotation matrices Ω_x become sufficiently small: $1 - \frac{1}{2} \text{Tr} \Omega_x < 10^{-6}$. The simulated annealing algorithm which we used is the following. The action (12) was multiplied by a factor γ (coupling constant) and then the quantum dynamics of variables $\{z_\alpha\}$ was simulated with the standard Metropolis algorithm. From the initial value $\gamma \approx 0.1$ the coupling constant was moved towards $\gamma = \infty$ with steps $\Delta\gamma = 0.1$. Fifteen thermalization steps were performed for each γ and the algorithm was stopped when the acceptance rate became smaller than 0.5%. After that on all plaquettes with $z_\alpha = -1$ the corresponding $\vec{n}_{i,\alpha}$, $i = 0, \dots, 3$ were inverted $\vec{n}_{i,\alpha} \rightarrow -\vec{n}_{i,\alpha}$.

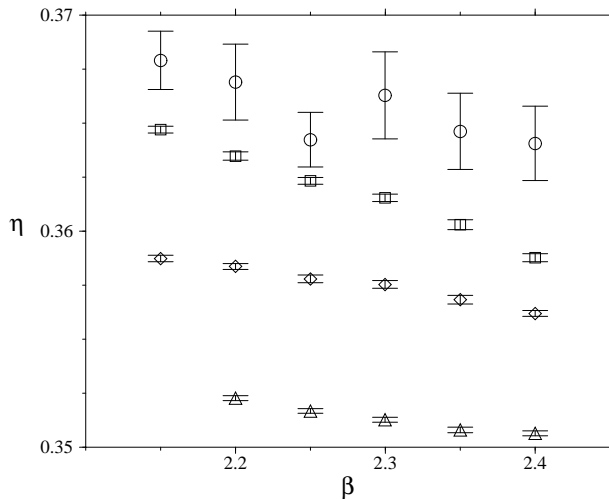


Fig. 8

To monitor the quality of each algorithm we consider

$$\eta = \frac{1}{2} (1 - \langle \vec{n}_{i,\alpha} \cdot \vec{n}_{j,\beta} \rangle), \quad (16)$$

where $\vec{n}_{i,\alpha} \cdot \vec{n}_{j,\beta}$ is the gauge invariant scalar product of two neighboring vectors. The dependence $\eta(\beta)$ on 12^4 lattice is presented on Fig. 8, where circles denote the local minimization without any preconditioning, while the local minimization with minimal Landau and Maximal Abelian gauge preconditioning are the squares and diamonds, respectively. Triangles are the results for the simulated annealing algorithm.

It should be noted that although the absolute values of η varies slightly for various algorithms, the corresponding monopole densities differ by an order of magnitude. Note also that in the case of Maximal Abelian gauge preconditioning there was in fact no local minimization at all (see section 4). Nevertheless the η values and monopole densities with MAA gauge are at least comparable with ones obtained via the simulated annealing.

Let us now turn to the physically interesting question about the monopole density. Fig. 9 represents the densities of artifacts (circles) and monopoles (squares) versus bare coupling constant β on a 14^4 lattice. In view of the above discussion of the monopole-artifact mixing it should not be a surprise that none of the graphs on Fig. 9 follows the renormalization group prediction

$$\rho_{lat} = \frac{\rho_{phys}}{4\Lambda^3} \left[\frac{6\pi^2}{11} \beta \right]^{153/121} \exp\left\{-\frac{9\pi^2}{11} \beta\right\}, \quad (17)$$

which is to be valid for physical monopoles. Moreover, Fig. 9 clearly confirms the actionless nature of artifacts since their density is almost constant in the whole range of β considered.

As we have already discussed, the monopole-artifact separation is *a priori* not a well defined procedure at a finite lattice spacing. Nevertheless, it is amusing to note that in case of $D = 4$ $SU(2)$ lattice gluodynamics the difference between the monopole and artifact

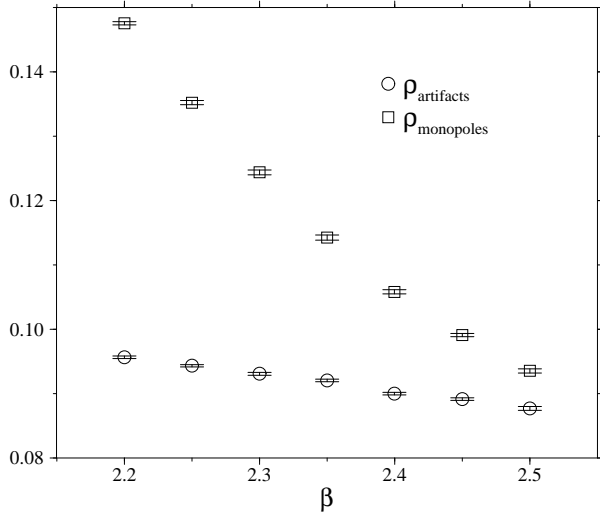


Fig. 9

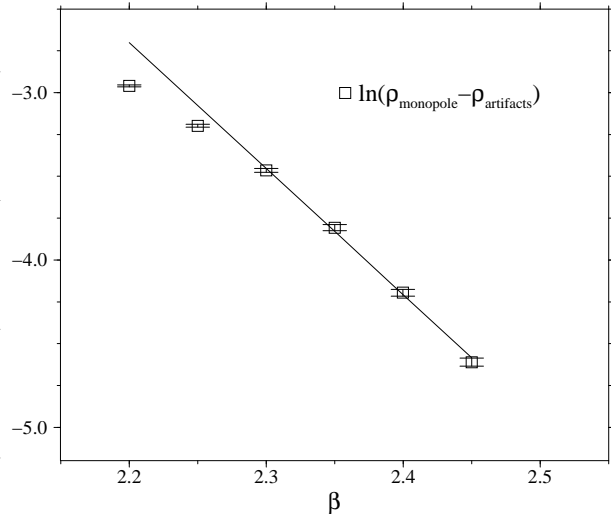


Fig. 10

densities follows Eq. (17) sharply, see Fig. 10. It seems so that in four dimensions and in the weak coupling regime artifacts do indeed form small dipoles with the monopoles living on the dual lattice. In this way one can explain the observed scaling behavior of $\rho_{phys} = \rho_{monopoles} - \rho_{artifacts}$ although there are strictly speaking no rigorous arguments why ρ_{phys} scales. Indeed, the monopole-artifact dipole picture is just an unproved assumption which, however, works unexpectedly well in $D = 4$ $SU(2)$ LGT. The rigorous artifact separation is still an unresolved problem which is beyond the scope of the present publication.

Assuming that the above dipole picture is valid one can estimate the density of the physical monopoles in the continuum limit. As follows from Fig. 10, $\ln \rho_{phys}/4\Lambda^3 \approx 11.9$ and using the numerical value of the string tension $a\sqrt{\sigma} = 0.1326$ at $\beta = 2.6$ (see, e.g. Ref [9]) one gets:

$$\rho_{phys} = (1.72 \sqrt{\sigma})^3 \approx (760 \text{ MeV})^3, \quad (18)$$

where the conventional value $\sqrt{\sigma} = 440 \text{ MeV}$ has been used.

Conclusions

We have implemented the gauge invariant monopole charge definition in the $SU(2)$ lattice gluodynamics. The lattice implementation is of particular importance since there are no analytical approaches to the gauge invariant monopoles in the continuum limit. Indeed, the corresponding classical Wu-Yang solution is unstable. Our lattice construction is based on the continuum definition of the monopole charge proposed recently and in fact follows it as close as possible. In this way we were able to obtain integer valued conserved monopole currents.

As might be expected, the lattice formulation brings in a set of specific problems. One of them is the appearance of the effective Ising model. In fact, the gauge invariance of monopoles on the lattice crucially depends on our ability to find its ground state, which is a non-trivial task because the model is frustrated. But at least in principle this

problem might be solved. Moreover, here we found a hint on the distinguished role of the Maximal Abelian gauge, which proved to be successful in the context of Abelian monopole confinement mechanism.

Another problem specific for the lattice is the emergence of the lattice artifacts. In more detail:

i) Artifacts are mixed up with physical monopoles. Thus it is necessary to subtract their contribution in order to get physical results. For simple quantities, like monopole density the artifact separation is indeed possible. Then the density of physical monopoles seems to scale correctly towards the continuum limit. However, it is not yet completely clear how to get rid of the artifacts in general case.

ii) Due to artifacts mixing the hypercubical geometry of the original lattice has to be changed. The monopole currents are still conserved, but the conservation takes place on a complicated lattice, the geometry of which is still not well understood. Probably the understanding of the lattice geometry will help to treat artifacts in a more rigorous way.

Acknowledgments.

We acknowledge thankfully the fruitful discussions with V. Belavin, M.N. Chernodub, R. Hofmann, M.I. Polikarpov, L. Stodolsky and V.I. Zakharov. The work was partially supported by grants RFFI-02-02-17308, RFFI-0015-96786, INTAS-00-0011 and CRDF award RP1-2364-MO-02.

References

- [1] F.V. Gubarev, V.I. Zakharov, '*Gauge Invariant Monopoles in SU(2) Gluodynamics*', hep-lat/0204017.
- [2] T.T. Wu, C.N. Yang, in *Properties of Matter Under Unusual Conditions*, ed. H. Mark and S. Fernback (New York, 1969).
- [3] T. Yoneya, *Phys. Rev.* **D8** (1977) 429;
R.A. Brandt, F. Neri, *Nucl. Phys.* **B161** (1979) 253-282.
- [4] M.N. Chernodub, F.V. Gubarev, M.I. Polikarpov, V.I. Zakharov, *Nucl. Phys.* **B600** (2001) 163-184, hep-th/0010265.
- [5] M. Luscher, *Comm. Math. Phys.* **85** (1982) 39;
P. Woit, *Nucl. Phys.* **B262** (1985) 284;
A. Phillips, D. Stone, *Comm. Math. Phys.* **103** (1986) 599-636; *Comm. Math. Phys.* **131** (1990) 255-282;
A.S. Kronfeld, M.L. Laursen, G. Schierholz, U.J. Wiese, *Nucl. Phys.* **B292** (1987) 330.
- [6] T.A. De Grand, D. Toussaint, *Phys. Rev.* **D22** (1980) 2478.

- [7] G.S. Bali, V. Bornyakov, M. Muller-Preussker, K. Schilling, *Phys. Rev.* **D54** (1996) 2863.
- [8] T.L. Ivanenko, A.V. Pochinsky, M.I. Polikarpov, *Phys. Lett.* **B252** (1990) 631-635.
- [9] M. Teper, '*Glueball masses and other physical properties of $SU(N)$ gauge theories in $D = 3 + 1$: a review of lattice results for theorists*', hep-th/9812187.